

---

# APPROACHING THE CONFORMAL LIMIT OF QUARK MATTER WITH DIFFERENT CHEMICAL POTENTIALS

---

**Connor Brown**

Center for Nuclear Research  
Kent State University  
Kent, OH 44242 USA  
cbrow232@kent.edu

**Veronica Dexheimer**

Center for Nuclear Research  
Kent State University  
Kent, OH 44242 USA  
vdexheim@kent.edu

**Rafael Bán Jacobsen**

Center of Natural and Exact Sciences  
Universidade Federal de Santa Maria  
Santa Maria, RS, Brazil  
rafaeljacobsen@gmail.com

**Ricardo Luciano Sonego Farias**

Center of Natural and Exact Sciences  
Universidade Federal de Santa Maria  
Santa Maria, RS, Brazil  
ricardo.farias@ufsm.br

## ABSTRACT

We study in detail the influence of different chemical potentials (baryon, charged, strange, and neutrino) on how and how fast a free gas of quarks in the zero-temperature limit reaches the conformal limit. We discuss the influence of non-zero masses, the inclusion of leptons, and different constraints, such as charge neutrality, zero-net strangeness, and fixed lepton fraction. We also investigate for the first time how the symmetry energy of the system under some of these conditions approaches the conformal limit. Finally, we briefly discuss what kind of corrections are expected from perturbative QCD as one goes away from the conformal limit.

**Keywords** Conformal limit · Quark matter · Chemical potential · Symmetry energy

## 1 Introduction and Formalism

In the zero temperature limit, baryons start to overlap at a few times saturation density and, through some mechanism that is not yet understood, quarks become effectively deconfined Baym et al. [2018]. In this work we discuss dense matter in terms of baryon chemical potential  $\mu_B$ , instead of baryon (number) density  $n_B$ , as the former (together with other chemical potentials, such as charged  $\mu_Q$  or strange  $\mu_S$ ) is the fixed or independent quantity in the grand canonical ensemble. The correspondence between  $n_B$  and  $\mu_B$  is model dependent, but, at finite temperature, the  $\mu_B$  at which deconfinement takes place is expected to be even lower (see e.g., Alford et al. [2008]), which highlights the importance of studying quark matter. We are particularly interested in understanding the conformal limit, the asymptotically high  $\mu_B$  at which matter can be described by a free (non-interacting) gas of massless quarks. For this reason, in the present work, we focus on modelling quark matter only and for the time being restrict ourselves to the zero-temperature limit.

To describe the quarks, we make use of a free Fermi gas under different assumptions. To start, we describe them simply by a massless gas, then introduce different non-zero quark masses, and vary independently the baryon, charged, and strange chemical potentials. We further link the chemical potentials by imposing charge neutrality and/or zero net strangeness. We also discuss the role played by leptons, discussing  $\beta$  equilibrium and the role played by neutrinos (with chemical potential  $\mu_\nu$ ). We investigate large  $\mu_B$  and different  $\mu_Q$  and  $\mu_\nu$ , as these are important for astrophysical scenarios, such as neutron stars and neutron-star mergers. On the other hand, we investigate the effects of  $\mu_S$ , which is important for discussions related to relativistic heavy-ion collisions and the early universe Letessier et al. [1995].

We also discuss the symmetry energy of quark matter for some of the constraints we study and investigate how it changes as we approach the conformal limit. Several works have addressed the symmetry energy of quark matter Chu and Chen [2014], Chen [2017], Wu et al. [2018], Thakur and Dhiman [2017]. This physical quantity is defined as the difference of energy per baryon  $E/N_B$  (or energy density per baryon density  $\varepsilon/n_B$ ) of fully isospin asymmetric

matter  $\delta = 1$  and isospin-symmetric matter  $\delta = 0$ :

$$E_{\text{sym}} = \frac{E_{\delta=1}}{N_B} - \frac{E_{\delta=0}}{N_B} = \frac{\varepsilon_{\delta=1}}{n_B} - \frac{\varepsilon_{\delta=0}}{n_B}, \quad (1)$$

where  $\delta$  was originally defined for matter with neutrons and protons in terms of densities  $n_i$  as

$$\delta = \frac{n_n - n_p}{n_n + n_p}. \quad (2)$$

In this case and also when one is considering up and down quarks,  $\delta$  can also be written as

$$\delta = -2Y_I = 1 - 2Y_Q \text{ (non - strange matter)}, \quad (3)$$

with fractions  $Y_i$  summing over  $i =$  baryons and/or quarks and defined in terms of particle isospin  $Q_{I_i}$  and electric charge  $Q_i$

$$Y_I = \frac{\sum_i Q_{I_i} n_i}{\sum_i n_i}, \quad Y_Q = \frac{\sum_i Q_i n_i}{\sum_i n_i}, \quad (4)$$

with baryon (number) density  $n_B = \sum n_i$ , where the quark densities are divided by 3.

However, it is important to note that, as discussed in Ref. Aryal et al. [2020] and Appendix A of Ref. Yao et al. [2023], in the presence of hyperons (or in our case strange quarks), Eq. (3) does not apply. For this reason, we restrain to the discussion of symmetry energy for the 2-flavor case (with up and down quarks).

When leptons are included, we assume  $\beta$  equilibrium, in which case electrons and muons have chemical potential  $\mu_e = \mu_\mu = -\mu_Q$ . In the special case that (electron and muon) neutrinos are trapped,  $\mu_\nu$  is determined by fixing the lepton fraction

$$Y_l = \frac{\sum_{lep} n_{lep}}{\sum_i n_i}, \quad (5)$$

usually hold equal to the canonical value 0.4, to simulate conditions created in supernova explosions Burrows and Lattimer [1986].

Finally, we briefly discuss the effects of interactions in the case that they are weak enough to be discussed perturbatively, i.e., using perturbative Quantum Chromodynamics, pQCD). At large temperatures and/or quark chemical potentials, the strong coupling becomes small enough to allow an infinite number of terms to be approximated by a finite number of terms to describe interactions Politzer [1973]. At zero temperature, pQCD corrections have been calculated up to next-to-next-to-next-to-leading order (N<sup>3</sup>LO) Gorda et al. [2021a,b] with non-zero quark masses included until next-to-next-to-leading order (N<sup>2</sup>LO) Kurkela et al. [2010], Graf et al. [2016], Gorda and Säppi [2022].

## 2 Results

We describe in detail the free Fermi gas formalism we use in this work (for quarks and leptons) in Appendix A. We begin our discussion by ignoring the contribution of leptons to the thermodynamical quantities (later we include different possibilities and discuss them). In the figures that follow, the pressure  $P$  and baryon density  $n_B$  are normalized by respective values of a free gas with the same number of quark flavors included, but with quark masses  $m_i = 0$  and  $\mu_Q = \mu_S = 0$ . Simple analytical equations for the pressure of all the massless cases discussed in this work are derived in Appendix B. We start our discussion considering only one chemical potential, and then expand our discussion to two and three chemical potentials.

### 2.1 One chemical potential $\mu_B$

We start by comparing the quark mass effect on  $n_B$  versus  $\mu_B$  in the left upper panel of Fig. 1. Because in this case  $\mu_Q$  and  $\mu_S$  are zero, all quarks present the same chemical potential  $\mu_i = \mu_u = \mu_d = \mu_s = \frac{1}{3}\mu_B$ . Due to our normalization (thermodynamical quantities divided by the massless case with the respective number of flavors), all massless cases have constant value 1. Nevertheless, this does not mean that they are the same (if not normalized). To discuss the effect of quark masses, we start with 1 flavor with mass corresponding to the Particle Data Group (PDG) Workman and Others [2022]) mass of the up ( $m = 2.3$  MeV) or down ( $m = 4.8$  MeV) quarks, then we look at the 2-flavor case with PDG masses for both light quarks. After that, we look at 3-flavors and use first only non-zero mass for the strange quark (with PDG value of  $m = 95$  MeV) and then the PDG (from hereon “realistic”) masses for the 3 quarks.

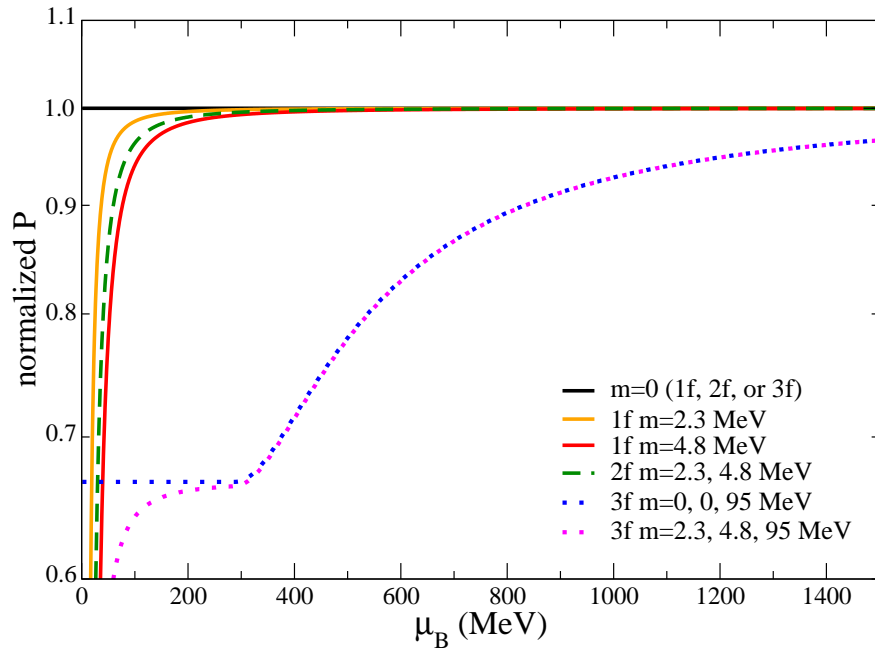
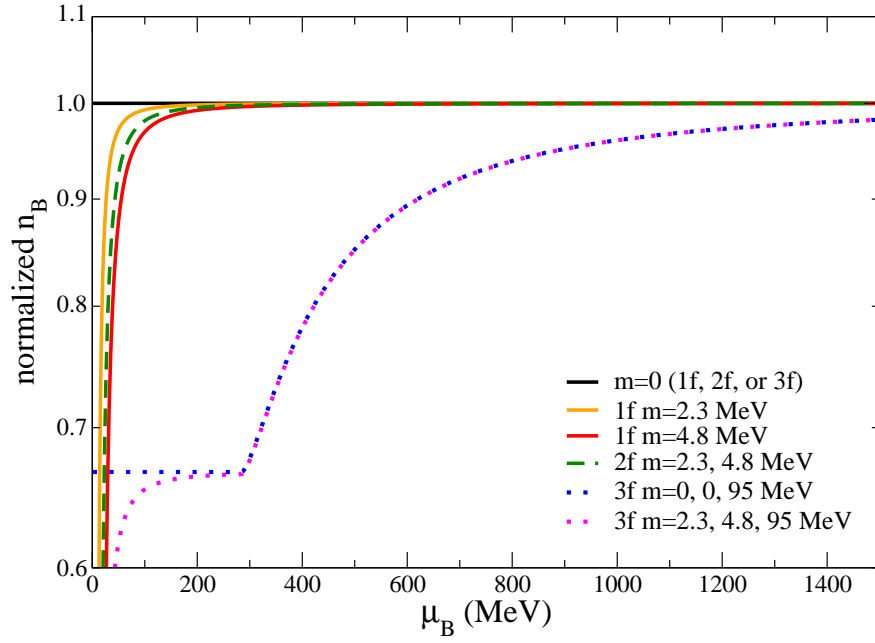


Figure 1: Baryon density (upper panel) and pressure (lower panel) of quarks with different number of flavors and different masses normalized by the respective massless cases.

We find that the introduction of realistic quark masses decreases the density for low  $\mu_B$ , with the s-quark mass affecting the density until larger  $\mu_B$  (up to 621 MeV) than the two light quarks (up to 55 MeV). To calculate these thresholds, we use throughout this paper the criteria of a deviation of 10% from the black line with value 1. For  $P$  versus  $\mu_B$ , shown in the lower panel of Fig. 1, the lines are very similar in shape (to the ones in the upper panel of the figure). The introduction of realistic quark masses decreases again  $P$  for low  $\mu_B$ , with the s-quark mass affecting the pressure until larger  $\mu_B$  (up to 834 MeV) than the two light quarks (up to 77 MeV).

## 2.2 Two chemical potentials $\mu_B$ and $\mu_Q$

Now, we abandon the unphysical 1-flavor case, and continue with 2- and 3-flavor cases. The 2-flavor case has recently become more relevant for dense matter because it has been shown that the core of neutron stars can harbor 3-, as well as 2-flavor quark matter Holdom et al. [2018]. For this case we add another (charged) chemical potential, breaking some of the degeneracy in the quark chemical potentials:  $\mu_{\text{up}} = \frac{1}{3}\mu_B + \frac{2}{3}\mu_Q$ ,  $\mu_{\text{down}} = \mu_{\text{strange}} = \frac{1}{3}\mu_B - \frac{1}{3}\mu_Q$ . Once more, we normalize thermodynamical quantities dividing by the respective values of the same quantity for a free gas with the same number of quark flavors included, but with  $m_i = 0$ , in addition to  $\mu_Q = 0$ . Following this procedure, we aim at determining how the conformal limit and its deviation depend on  $\mu_Q$ .

When  $\mu_Q$  is determined by charge neutrality, the results even for the massless case depend on the number of flavors. In this case, only the 3-flavor case is coincidentally equal to the  $\mu_Q = 0$  case (see the explanation following Eqs. (34) to (37) in Appendix B). For 2-flavor, this is not the case, and the pressure is lower than in the  $\mu_Q = 0$  case, establishing a new lower conformal limit (see upper panel of Fig. 2). Expressions for the pressure for each particular chemical potential case (always keeping  $m_i = 0$  for simplicity) can be found in Appendix B. Compare e.g., Eqs. (22) and (31). When adding quark masses,  $\mu_Q$  determined by charge neutrality lowers the pressure (in comparison to the respective massless case and to the massless case with  $\mu_Q = 0$ ) such that it goes to the respective conformal limit at larger  $\mu_B$ . Using again the criteria of 10% deviations from the respective conformal limit, the s-quark mass affects pressure until  $\mu_B = 839$  MeV and the two light quark masses until  $\mu_B = 118$  MeV.

Nevertheless, one issue about this approach should be noted: we are comparing very small values of  $\mu_Q$  with very large values of  $\mu_B$ . See the middle panel of Fig. 2 for a comparison. This is particularly the case for 3-flavors of quarks, and (except for extremely low  $\mu_B$ ) this behavior is independent of the quark masses. For small values of  $\mu_B$ , both for 2 and 3-flavors, the dependence of  $\mu_Q$  and  $\mu_B$  can be predicted in fair agreement with Eq. (30). For this reason, next, we add a fixed charged chemical potential to study how it affects the conformal limit, which translates into an increase in pressure (see e.g., the different lines for 3-flavor quark matter with realistic masses in the lower panel of Fig. 2), specially at low values of  $\mu_B$ . For massless quarks and  $\mu_Q = -20$  MeV, the pressure is always above the conformal limit for  $\mu_Q = 0$ , independently of the number of flavors. Once the quark masses are finite, the pressure decreases, specially in the 3-flavor case. For larger absolute values of  $\mu_Q$ , the pressure becomes larger, even going above the conformal case (with and without  $\mu_Q$ ). For example, for the 3-flavor case with realistic quark masses and  $\mu_Q = -50$  MeV, the pressure deviates 10% (of the  $\mu_Q = 0$  conformal limit) at  $\mu_B = 698$  MeV and for  $\mu_Q = -100$  MeV at  $\mu_B = 415$  MeV (the latter one from above). Finally, there is one important remark regarding the behavior of the normalized pressure: in the lower panel of Fig. 2, it is shown that this physical quantity decreases for small values of  $\mu_B$ ; however, this behavior doesn't mean that the pressure itself (not normalized) is not a monotonically increasing function of  $\mu_B$ . Here, we must remember that our normalization is carried out by dividing the thermodynamical quantities (such as pressure) by the massless case with the respective number of flavors, and the free Fermi pressure of this system of massless quarks used for normalization scales as  $\mu_B^4$ ; therefore, in those ranges of  $\mu_B$  where  $P$  for massive quarks increases at a lower rate than  $\mu_B^4$ , the normalized pressure decreases without implying any thermodynamical inconsistency.

## 2.3 Three chemical potentials $\mu_B$ , $\mu_Q$ , and $\mu_S$ or $\mu_\nu$

Going further, we can add another (strange) chemical potential and constrain it, e.g., to strangeness neutrality. The issue is that at zero temperature strangeness neutrality means that there are no strange quarks, and the 3-flavor reduces to the 2-flavor case. For this reason, we fixed  $\mu_S$  instead to specific values.  $\mu_S$  breaks the degeneracy in the remaining quark chemical potentials:  $\mu_{\text{up}} = \frac{1}{3}\mu_B + \frac{2}{3}\mu_Q$ ,  $\mu_{\text{down}} = \frac{1}{3}\mu_B - \frac{1}{3}\mu_Q$ ,  $\mu_{\text{strange}} = \frac{1}{3}\mu_B - \frac{1}{3}\mu_Q + \mu_S$ . Once more, we normalize thermodynamical quantities dividing by the respective values of the same quantity for a free gas with the same number of quark flavors included, but with  $m_i = 0$ , in addition to  $\mu_Q = 0$ .

Fixing  $\mu_S$  increases the pressure, similar to fixing  $\mu_Q$ . Compare, for example, the massless 3-flavor case in the upper panel in Fig. 3 and lower panel in Fig. 2 and note that the pressure for a given  $\mu_B$  is now much higher. When quark masses are added, the similarity disappears, because  $\mu_S$  only affects the strange quarks, which do not appear for low values of  $\mu_B$ , unless the  $\mu_S$  value is larger than the strange quark mass, which corresponds to our case of  $\mu_S = 100$

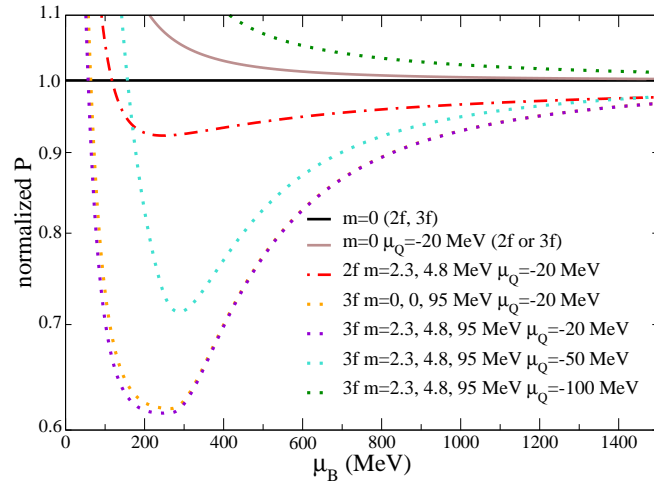
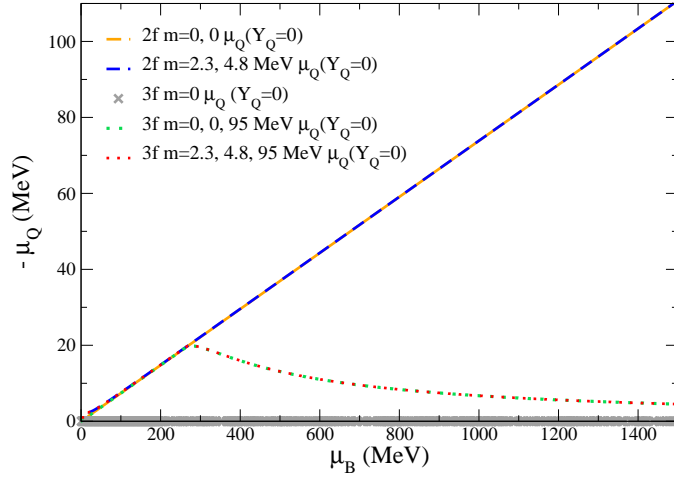
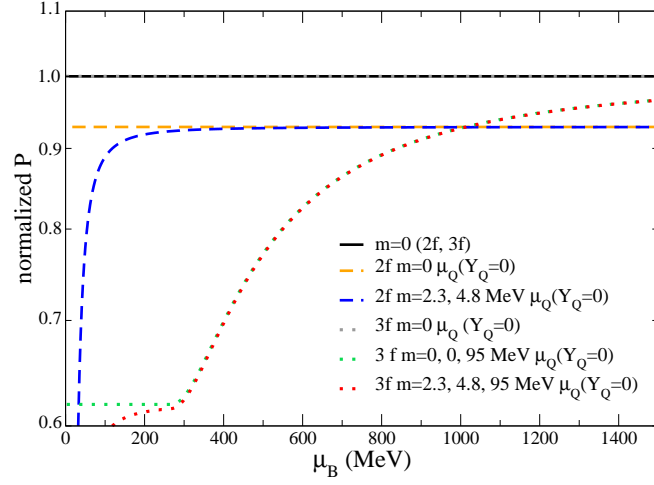


Figure 2: Pressure (upper panel) and charged chemical potential (middle panel) of quarks with 2 chemical potentials normalized by the respective massless case with one chemical potential,  $\mu_B$ . The charged chemical potential is determined by charge neutrality. For massless 3-flavor quarks, the cases with and without  $\mu_Q$  coincide. Lower panel: Pressure of quarks with 2 chemical potentials, being  $\mu_Q$  fixed to different values, normalized by the respective massless case with one chemical potential,  $\mu_B$ .

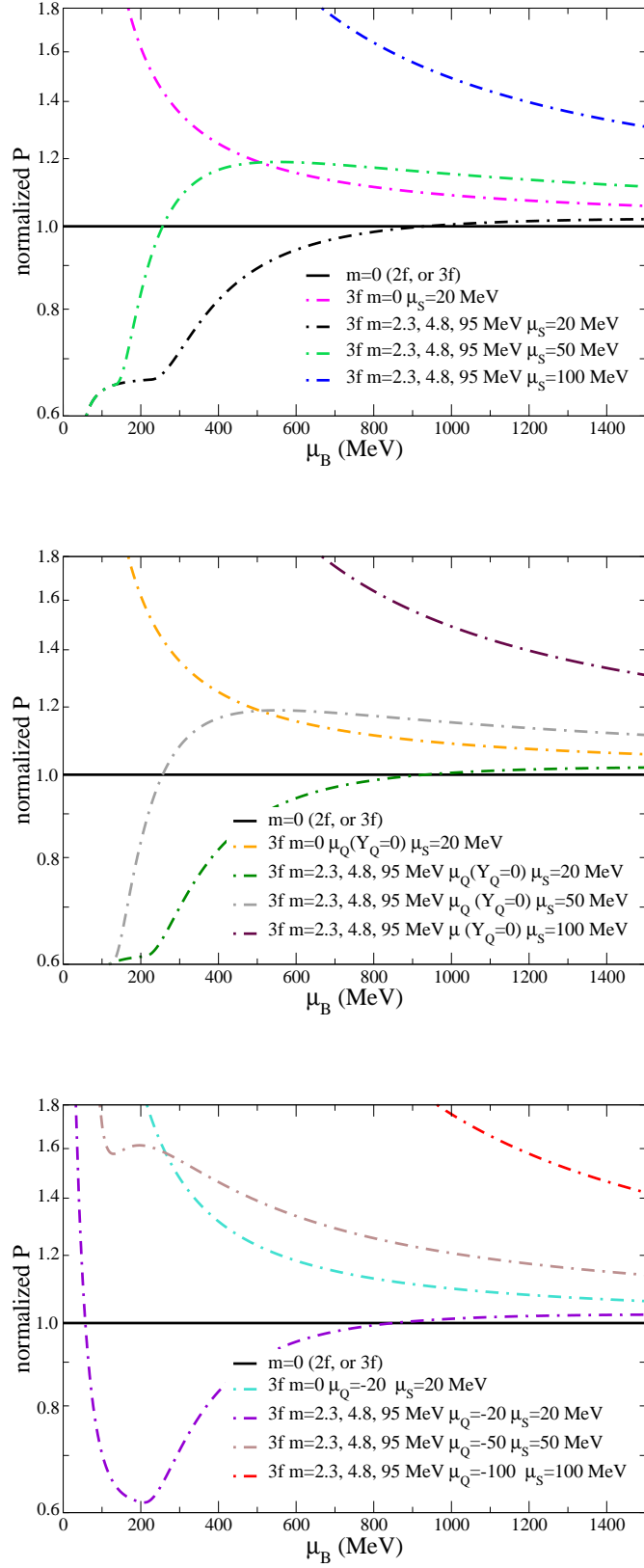


Figure 3: Pressure and charged chemical potential of quarks with 2 or 3 chemical potentials, including the strange chemical potential, normalized by the respective massless case (with one chemical potential,  $\mu_B$ ). The charged chemical potential is either zero (upper panel), determined by charge neutrality (middle panel), or fixed (lower panel). For massless 3-flavor quarks, the cases with charge neutrality and without  $\mu_Q$  coincide.

MeV. For  $\mu_S = 50$  and  $\mu_S = 100$  MeV, the 10% deviation from the conformal limit takes place at  $\mu_B = 1743$  and  $\mu_B = 4227$  MeV, respectively (both from above).

Now we consider the case in which additionally  $\mu_Q \neq 0$ , determined to reproduce charge neutrality (middle panel of Fig. 3). For massless 3-flavor quarks, the cases with charge neutrality and without  $\mu_Q$  coincide. When masses are introduced, the curves are still very similar (to the upper panel for the  $\mu_Q = 0$  case), except at very small  $\mu_B$ , where the quark masses are comparable to both  $\mu_B$  and  $\mu_Q$ . For  $\mu_S = 50$  and  $\mu_S = 100$  MeV, the 10% deviation from the conformal limit takes place at  $\mu_B = 1743$  and  $\mu_B = 4227$  MeV, respectively (both from above). When a fixed value of  $\mu_Q$  is used, it increases the pressure further, specifically at low  $\mu_B$  (see lower panel of Fig. 3). For  $\mu_Q = \mu_S = 50$  and  $\mu_Q = \mu_S = 100$  MeV, the 10% deviation from the conformal limit takes place at  $\mu_B = 2070$  and  $\mu_B = 4723$  MeV, respectively (both from above).

Next, we investigate the effects of having much larger values of  $\mu_Q$  and  $\mu_S$ , comparable to  $\mu_B$ , for 3 flavors of quarks in the upper panel of Fig. 4. As expected, the changes due to the additional chemical potentials take place at much lower  $\mu_B$  (notice the different scale in the y-axis of the figure) and practically all the curves are above the one chemical potential ( $\mu_B$ ) conformal limit. An exception is the case with large (negative)  $\mu_Q$  (and  $\mu_S = 0$ ) because, according to Eqs. 6 and 10, quarks can only exist after a given  $\mu_B = 381$  MeV, at which the momentum  $k_i$  and  $P$  become finite (see Eq. 33 for the massless case). In this case, the pressure differs from the one chemical potential conformal limit by more than 10% until  $\mu_B = 10\,583$  MeV. In the case of large  $\mu_S$ , quarks can exist at any  $\mu_B$  and the pressure differs from the one chemical potential conformal limit by more than 10% until  $\mu_B = 44\,237$  MeV. When we combine large  $\mu_S$  and (absolute value of)  $\mu_Q$ , the pressure differs from the one chemical potential conformal limit by more than 10% until  $\mu_B = 48\,897$  MeV. In this case, the curve in the upper panel of Fig. 4 begins only at  $\mu_B = 1000$  MeV. This can be understood once more from Eqs. 6 and 10. The same effect can also be seen (although more subtle) in the bottom panel of Fig. 2, where the fixed  $\mu_Q$  cases start at  $\mu_B = -\mu_Q$ .

Finally, we investigate changes due to the inclusion of a free gas of leptons (electrons and muons) in  $\beta$  equilibrium (and participating in the fulfillment of charge neutrality). As it can be seen in the lower panel of Fig. 4, the inclusion of leptons doesn't change the pressure. The picture changes though when lepton number is fixed. In this case, which also includes neutrinos, the pressure is considerably higher because the large amount of negative leptons forces the appearance of a large amount of up quarks, changing considerably the quark composition of the system. The grey full line shows a kink for  $\mu_B \sim 400$  MeV, when the muons appear. Note that the difference in massless versus massive quarks is still very pronounced when  $Y_l$  is fixed.

## 2.4 Symmetry energy

As already discussed, we calculate the symmetry energy only for the 2-flavor case, for which it was originally defined. We fix  $n_B$  in this case (instead of  $\mu_B$  as we have been doing) because the symmetry energy is defined for a given  $n_B$ , but limit the x-axis to approximately the corresponding range from the previous figures. Fig. 5 shows that the curves are a monotonically increasing function of density. The light quark masses don't affect the results. Notice that the latter statement applies to every thermodynamical quantity that is not normalized by the respective conformal limit (and does not include derivatives). Numerically, we define  $\delta = 0$  as the 2-flavor  $\mu_Q = 0$  case (corresponding to the 2-flavor lines in Fig. 1) and  $\delta = 1$  as the 2-flavor  $Y_Q = 0$  case (with  $\mu_Q \neq 0$  corresponding to the 2-flavor lines in the top and middle panels of Fig. 2).

## 3 Discussion and Conclusions

Perturbative corrections to a free gas of quarks due to interactions always bring down the pressure to lower values. Although these corrections have been calculated to higher orders for massless and massive (strange) quarks, they cannot accurately be carried out to low baryon chemical potentials  $\mu_B$  (or, interchangeably, low baryon densities  $n_B$  in the zero-temperature limit). For example, for the relevant regime of densities inside neutron stars,  $\mu_B \leq 1500$  MeV, pQCD predicts that the pressure is lower than 80% of the free gas value (see for example Fig. 1 of Ref. Graf et al. [2016]) but with a very large band going all the way to  $P = 0$ .

In this work, we have investigated the equation of state of a free gas of quarks focusing on how the conformal limit is reached when different chemical potentials are varied and different constraints (e.g., for laboratory vs. astrophysics) are considered. This is done by using combinations of 1, 2, or 3 chemical potentials out of the 4 we consider, each related to a possible conserved quantity: baryon number  $B$  ( $\mu_B$ ), electric charge ( $\mu_Q$ ), strangeness ( $\mu_S$ ), and lepton number ( $\mu_\nu$ ). We have also derived expressions for massless quarks under different conditions to illustrate our discussion.

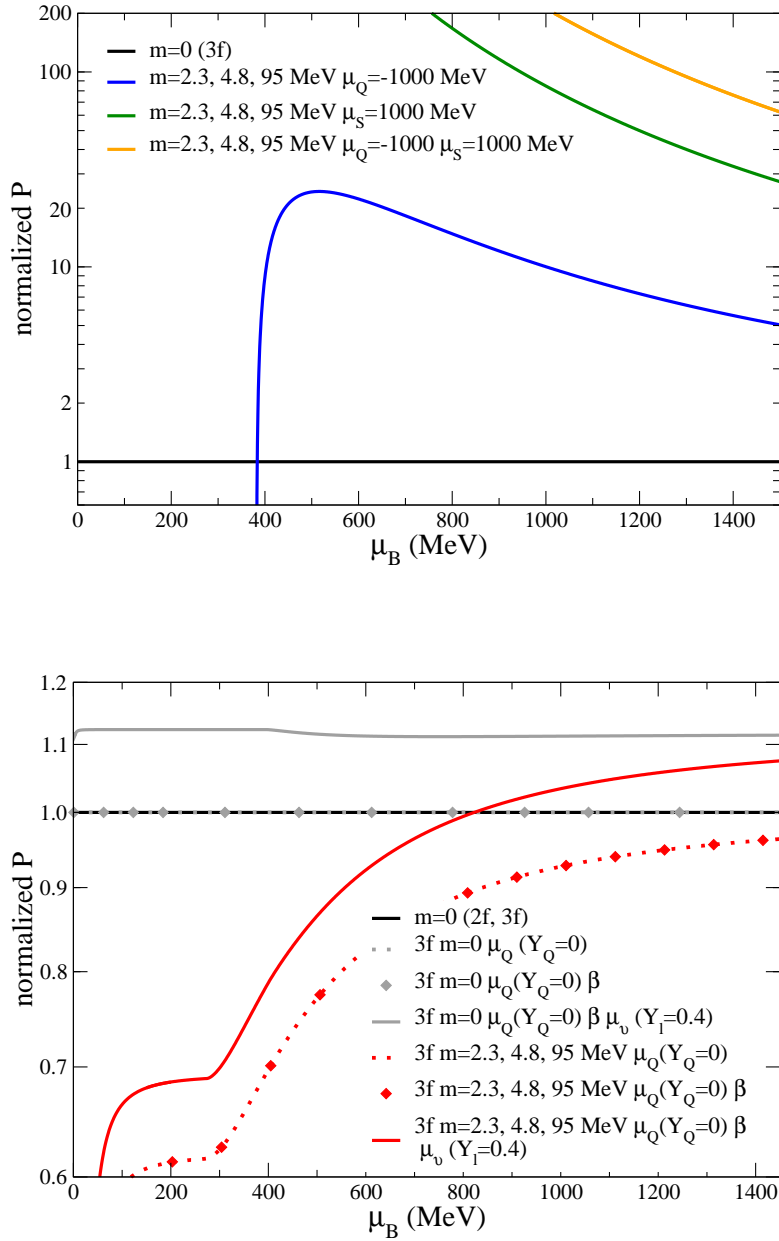


Figure 4: Upper panel: Pressure of quarks with 2 or 3 large chemical potentials, normalized by the respective massless case with one chemical potential,  $\mu_B$ . Lower panel: Pressure of quarks and leptons with 2 or 3 chemical potentials, normalized by the respective massless case with one chemical potential,  $\mu_B$ . For  $\beta$ -equilibrium with leptons,  $\mu_Q$  is determined by charge neutrality. When neutrinos are present, their chemical potential  $\mu_\nu$  is determined by fixing the lepton fraction,  $Y_l$ .



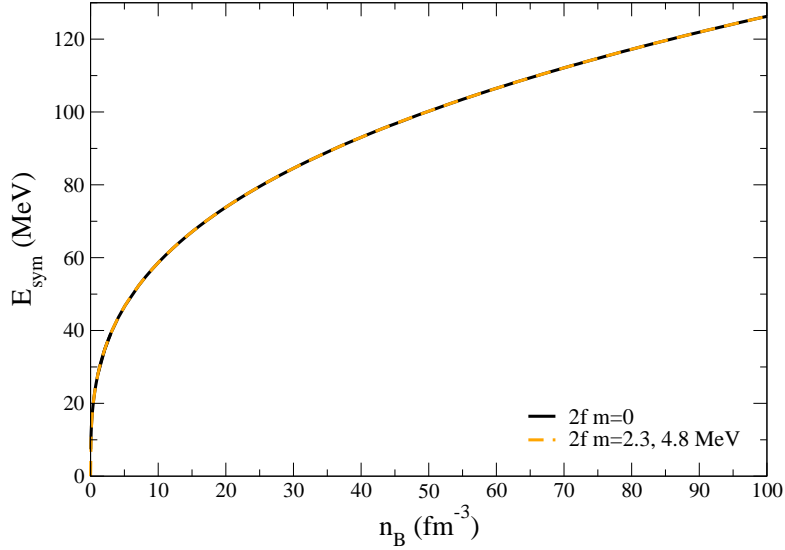


Figure 5: Symmetry energy of quarks with 1 or 2 chemical potentials as a function of baryon density for different masses. The two curves overlap.

We have studied the effects of using different quark masses (including PDG values), number of flavors, and different ways to fix the various chemical potentials considered. The latter procedure implies enforcing charge neutrality and, when leptons were included,  $\beta$  equilibrium. When leptons (electrons, muons, and their respective neutrinos) are present, the pressure is not altered. An exception is the case in which the lepton fraction is fixed. For different cases, we have quantified the deviation from the one-chemical potential (massless) conformal limit by verifying at which  $\mu_B$  the pressure deviates by more than 10%. This value varied from  $\mu_B = 77$  to 48 897 MeV. This shows that one must be careful about making statements concerning comparisons with "the" conformal limit. Finally, we have shown that the conformal limit of the symmetry energy is monotonically increasing and does not depend on quark masses.

## Acknowledgements

We acknowledge support from the National Science Foundation under grants PHY1748621, MUSES OAC2103680, and NP3M PHY-2116686. C. B. acknowledges support from the Kent State University SURE program. This work was partially supported by Conselho Nacional de Desenvolvimento Científico e Tecnológico (CNPq), Grant No. 312032/2023-4 (R.L.S.F.) and is also part of the project Instituto Nacional de Ciência e Tecnologia - Física Nuclear e Aplicações (INCT - FNA), Grant No. 464898/2014-5 (R.L.S.F.).

## A Appendix: General Expressions

For each quark flavor  $i$ , we can write

$$\mu_i = \frac{1}{3}\mu_B + Q_i\mu_Q + Q_{S_i}\mu_S, \quad (6)$$

where  $1/3$  has been used as the baryon number and  $Q_i$  and  $Q_{S_i}$  are the electric charge and strangeness of each quark.  $\mu_B$ ,  $\mu_Q$ , and  $\mu_S$  are the baryon, charged, and strange independent chemical potentials of the system. In our formalism, the isospin chemical potential  $\mu_I = \mu_Q$  Aryal et al. [2020].

The general expressions for (number) density, energy density and pressure of a relativistic free Fermi gas of particles  $i$  using the natural system of units are

$$n_i = \frac{g_i}{2\pi^2} \int_0^\infty dk_i k_i^2 (f_{i+} - f_{i-}), \quad (7)$$

$$\varepsilon_i = \frac{g_i}{2\pi^2} \int_0^\infty dk_i E_i k_i^2 (f_{i+} + f_{i-}), \quad (8)$$

$$P_i = \frac{1}{3} \frac{g_i}{2\pi^2} \int_0^\infty dk_i \frac{k_i^4}{E_i} (f_{i+} + f_{i-}), \quad (9)$$

where  $g_i = 6$  is the spin and color degeneracy factor,  $k_i$  is the momentum,

$$E_i = \sqrt{k_i^2 + m_i^2} \geq 0, \quad (10)$$

is the energy of the state,  $m_i$  the mass,  $f_\pm$  the distribution function of particles and antiparticles  $f_{i\pm} = (e^{(E_i \mp \mu_i)/T} + 1)^{-1}$ , with  $\mu_i$  being the particle chemical potential, and  $T$  the temperature.

In the  $T = 0$  limit, antiparticles provide no contribution,  $f_- = 0$ , and  $f_+ = 1$  up to the Fermi momentum,  $k_i = k_{F_i}$ ,  $E_i = \mu_i$  and the integrals for the above thermodynamic quantities are evaluable analytically

$$n_i = \frac{g_i}{6\pi^2} k_{F_i}^3, \quad (11)$$

$$\varepsilon_i = \frac{g_i}{2\pi^2} \left[ \left( \frac{1}{8} m_i^2 k_{F_i} + \frac{1}{4} k_{F_i}^3 \right) \sqrt{m_i^2 + k_{F_i}^2} - \frac{1}{8} m_i^4 \ln \frac{k_{F_i} + \sqrt{m_i^2 + k_{F_i}^2}}{m_i} \right], \quad (12)$$

$$P_i = \frac{1}{3} \frac{g_i}{2\pi^2} \left[ \left( \frac{1}{4} k_{F_i}^3 - \frac{3}{8} m_i^2 k_{F_i} \right) \sqrt{m_i^2 + k_{F_i}^2} + \frac{3}{8} m_i^4 \ln \frac{k_{F_i} + \sqrt{m_i^2 + k_{F_i}^2}}{m_i} \right]. \quad (13)$$

## B Appendix: Massless Quarks

For the massless particle case, the expressions above further reduce to

$$n_i = \frac{g_i}{6\pi^2} k_{F_i}^3 = \frac{g_i}{6\pi^2} \mu_i^3, \quad (14)$$

$$\varepsilon_i = \frac{g_i}{8\pi^2} k_{F_i}^4 = \frac{g_i}{8\pi^2} \mu_i^4, \quad (15)$$

$$P_i = \frac{1}{3} \frac{g_i}{8\pi^2} k_{F_i}^4 = \frac{1}{3} \frac{g_i}{8\pi^2} \mu_i^4, \quad (16)$$

reproducing  $\varepsilon_i = 3P_i$ .

Note that, in the case of massless free quarks, we can also write  $\mu_i = k_i$ . Therefore, we can write the chemical potential for each quark flavor using Eq. (6)

$$\mu_u = \frac{1}{3} \mu_B + \frac{2}{3} \mu_Q = k_u, \quad (17)$$

$$\mu_d = \frac{1}{3} \mu_B - \frac{1}{3} \mu_Q = k_d, \quad (18)$$

$$\mu_s = \frac{1}{3} \mu_B - \frac{1}{3} \mu_Q + \mu_S = k_s. \quad (19)$$

We use the convention that both the strangeness and  $\mu_S$  are positive. Alternatively, one could use both as negative without changing the results. Eqs. 17, and 18 are equal if  $\mu_Q = 0$ . Eqs. 17, 18, and 19 are equal if  $\mu_Q = 0$  and  $\mu_S = 0$ . The density and pressure of each quark flavor can be written further as

$$n_i = \frac{\mu_i^3}{\pi^2} = \frac{k_i^3}{\pi^2}, \quad (20)$$

$$P_i = \frac{\mu_i^4}{4\pi^2} = \frac{k_i^4}{4\pi^2}. \quad (21)$$

Next, we discuss the pressure for specific conditions concerning number of flavors and chemical potential constraints (not including leptons):

- 2-flavor,  $\mu_Q = 0$

$$P = P_u + P_d = 2P_u = \frac{2\mu_u^4}{4\pi^2} = \frac{\mu_B^4}{162\pi^2} = \frac{\mu_B^4}{1598.88}. \quad (22)$$

- 3-flavor,  $\mu_Q = 0, \mu_S = 0$

$$P = P_u + P_d + P_s = 3P_u = \frac{3\mu_u^4}{4\pi^2} = \frac{\mu_B^4}{108\pi^2} = \frac{\mu_B^4}{1065.92}. \quad (23)$$

- 2-flavor,  $\mu_Q$  fixed

$$\begin{aligned} P = P_u + P_d &= \frac{1}{4\pi^2} (\mu_u^4 + \mu_d^4) = \frac{1}{4\pi^2} \left[ \left( \frac{1}{3}\mu_B + \frac{2}{3}\mu_Q \right)^4 + \left( \frac{1}{3}\mu_B - \frac{1}{3}\mu_Q \right)^4 \right] \\ &= \frac{1}{4\pi^2} \left( \frac{\mu_B^4}{81} + \frac{4\mu_B^3}{27} \frac{2\mu_Q}{3} + \frac{6\mu_B^2}{9} \frac{4\mu_Q^2}{9} + \frac{4\mu_B}{3} \frac{8\mu_Q^3}{27} + \frac{16\mu_Q^4}{81} \right. \\ &\quad \left. + \frac{\mu_B^4}{81} - \frac{4\mu_B^3}{27} \frac{\mu_Q}{3} + \frac{6\mu_B^2}{9} \frac{\mu_Q^2}{9} - \frac{4\mu_B}{3} \frac{\mu_Q^3}{27} + \frac{\mu_Q^4}{81} \right) \\ &= \frac{1}{324\pi^2} [2\mu_B^4 + 4\mu_B^3\mu_Q + 30\mu_B^2\mu_Q^2 + 28\mu_B\mu_Q^3 + 17\mu_Q^4]. \end{aligned} \quad (24)$$

- 2-flavor,  $\mu_Q$  from charge neutrality

Starting from  $\sum_i Q_i n_i = 0$

$$\frac{2}{3}n_u - \frac{1}{3}n_d = 0, \quad (25)$$

$$\frac{2}{3} \frac{\mu_u^3}{\pi^2} - \frac{1}{3} \frac{\mu_d^3}{\pi^2} = 0, \quad (26)$$

$$2\mu_u^3 = \mu_d^3, \quad (27)$$

$$2 \left( \frac{1}{3}\mu_B + \frac{2}{3}\mu_Q \right)^3 = \left( \frac{1}{3}\mu_B - \frac{1}{3}\mu_Q \right)^3, \quad (28)$$

$$2^{\frac{2}{3}} \frac{1}{3}\mu_B - \frac{1}{3}\mu_B = -2^{\frac{1}{3}} \frac{2}{3}\mu_Q - \frac{1}{3}\mu_Q, \quad (29)$$

$$\mu_Q = \frac{-\left(2^{\frac{1}{3}} - 1\right)\mu_B}{2^{\frac{4}{3}} + 1} = -0.07 \mu_B. \quad (30)$$

We can then use Eqs. 27 and 30 to calculate the pressure

$$\begin{aligned} P &= P_u + P_d = \frac{1}{4\pi^2} (\mu_u^4 + \mu_d^4) = \frac{1}{4\pi^2} (\mu_u^4 + 2^{\frac{4}{3}}\mu_u^4) \\ &= \frac{1}{4\pi^2} (1 + 2^{\frac{4}{3}}) \mu_u^4 = \frac{1}{4\pi^2} (1 + 2^{\frac{4}{3}}) \left( \frac{1}{3}\mu_B + \frac{2}{3}\mu_Q \right)^4 \\ &= \frac{1}{4\pi^2} (1 + 2^{\frac{4}{3}}) \left[ \frac{1}{3}\mu_B - \frac{2}{3} \left( \frac{2^{\frac{1}{3}} - 1}{2^{\frac{4}{3}} + 1} \mu_B \right) \right]^4 \\ &= \frac{1}{4\pi^2} (1 + 2^{\frac{4}{3}}) \left[ \frac{2^{\frac{4}{3}} + 1 - 2^{\frac{4}{3}} + 2}{3(2^{\frac{4}{3}} + 1)} \right]^4 \mu_B^4 \\ &= \frac{1}{4\pi^2 (2^{\frac{4}{3}} + 1)^3} \mu_B^4 = \frac{\mu_B^4}{1721.59}. \end{aligned} \quad (31)$$

- 3-flavor,  $\mu_Q$  fixed,  $\mu_S = 0$

$$P = P_u + P_d + P_s = \frac{1}{4\pi^2} (\mu_u^4 + \mu_d^4 + \mu_s^4) = \frac{1}{4\pi^2} (\mu_u^4 + 2\mu_d^4), \quad (32)$$

because  $\mu_d = \mu_s$  are equal, resulting in

$$\begin{aligned}
P &= \frac{1}{4\pi^2} \left[ \left( \frac{1}{3}\mu_B + \frac{2}{3}\mu_Q \right)^4 + 2 \left( \frac{1}{3}\mu_B - \frac{1}{3}\mu_Q \right)^4 \right] \\
&= \frac{1}{4\pi^2} \left( \frac{\mu_B^4}{81} + \frac{4\mu_B^3}{27} \frac{2\mu_Q}{3} + \frac{6\mu_B^2}{9} \frac{4\mu_Q^2}{9} + \frac{4\mu_B}{3} \frac{8\mu_Q^3}{27} + \frac{16\mu_Q^4}{81} \right. \\
&\quad \left. + 2 \frac{\mu_B^4}{81} - 2 \frac{4\mu_B^3}{27} \frac{\mu_Q}{3} + 2 \frac{6\mu_B^2}{9} \frac{\mu_Q^2}{9} - 2 \frac{4\mu_B}{3} \frac{\mu_Q^3}{27} + 2 \frac{\mu_Q^4}{81} \right) \\
&= \frac{1}{324\pi^2} (3\mu_B^4 + 36\mu_B^2\mu_Q^2 + 24\mu_B\mu_Q^3 + 18\mu_Q^4) .
\end{aligned} \tag{33}$$

- 3-flavor,  $\mu_Q$  from charge neutrality,  $\mu_S = 0$

Starting again from  $\sum_i Q_i n_i = 0$

$$\frac{2}{3}n_u - \frac{1}{3}n_d - \frac{1}{3}n_s = 0, \tag{34}$$

$$\frac{2}{3} \left( \frac{\mu_u^3}{\pi^2} \right) - \frac{1}{3} \left( \frac{\mu_d^3}{\pi^2} \right) \frac{1}{3} - \left( \frac{\mu_s^3}{\pi^2} \right) = 0, \tag{35}$$

$$2\mu_u^3 - \mu_d^3 - \mu_s^3 = 0, \tag{36}$$

but, since in this case  $\mu_d = \mu_s$ , we have:

$$\mu_u^3 = \mu_d^3, \tag{37}$$

which implies (from Eqs. 17 and 18)  $\mu_Q = 0$  and reproduces the 3-flavor case with  $\mu_Q = 0, \mu_S = 0$ .

- 3-flavor, zero net strangeness

Starting from  $\sum Q_{S_i} n_i = 0$ , at  $T = 0$  this implies  $n_s = 0$ , no matter if  $\mu_Q = 0$  or  $\mu_Q \neq 0$ . As a consequence, this case reproduces the respective 2-flavor case.

- 3-flavor,  $\mu_Q$  fixed,  $\mu_S$  fixed

$$\begin{aligned}
P &= P_u + P_d + P_s = \frac{1}{4\pi^2} (\mu_u^4 + \mu_d^4 + \mu_s^4) \\
&= \frac{1}{4\pi^2} \left[ \left( \frac{1}{3}\mu_B + \frac{2}{3}\mu_Q \right)^4 + \left( \frac{1}{3}\mu_B - \frac{1}{3}\mu_Q \right)^4 + \left( \frac{1}{3}\mu_B - \frac{1}{3}\mu_Q + \mu_S \right)^4 \right].
\end{aligned} \tag{38}$$

Using the result from Eq. 33

$$\begin{aligned}
P &= \frac{1}{324\pi^2} (3\mu_B^4 + 36\mu_B^2\mu_Q^2 + 24\mu_B\mu_Q^3 + 18\mu_Q^4) \\
&\quad + \frac{1}{4\pi^2} \left( \mu_S^4 - \frac{4}{27}\mu_Q^3\mu_S - \frac{4}{3}\mu_Q\mu_S^3 + \frac{4}{3}\mu_B\mu_S^3 + \frac{4}{27}\mu_B^3\mu_S \right. \\
&\quad \left. + \frac{6}{9}\mu_Q^2\mu_S^2 + \frac{6}{9}\mu_B^2\mu_S^2 - \frac{12}{27}\mu_B^2\mu_Q\mu_S + \frac{12}{27}\mu_B\mu_Q^2\mu_S - \frac{12}{9}\mu_B\mu_Q\mu_S^2 \right).
\end{aligned} \tag{39}$$

- 3-flavor  $\mu_Q = 0, \mu_S$  fixed

Using Eq. 39 with  $\mu_Q = 0$

$$P = \frac{1}{\pi^2} \left( \frac{1}{108}\mu_B^4 + \frac{\mu_S^4}{4} + \frac{1}{3}\mu_B\mu_S^3 + \frac{1}{27}\mu_B^3\mu_S + \frac{1}{6}\mu_B^2\mu_S^2 \right). \tag{40}$$

- 3-flavor,  $\mu_Q$  from charge neutrality,  $\mu_S$  fixed

Starting from  $\sum Q_i n_i = 0$

$$\frac{2}{3}n_u - \frac{1}{3}n_d - \frac{1}{3}n_s = 0, \quad (41)$$

$$2\mu_u^3 - \mu_d^3 - \mu_s^3 = 0, \quad (42)$$

$$2 \left( \frac{1}{3}\mu_B + \frac{2}{3}\mu_Q \right)^3 - \left( \frac{1}{3}\mu_B - \frac{1}{3}\mu_Q \right)^3 - \left( \frac{1}{3}\mu_B - \frac{1}{3}\mu_Q + \mu_S \right)^3 = 0, \quad (43)$$

$$\begin{aligned} & \frac{2\mu_B^3}{27} + \frac{12\mu_B^2\mu_Q}{27} + \frac{24\mu_B\mu_Q^2}{27} + \frac{16\mu_Q^3}{27} - \frac{2\mu_B^3}{27} + \frac{6\mu_B^2\mu_Q}{27} - \frac{6\mu_B\mu_Q^2}{27} \\ & + \frac{2\mu_Q^3}{27} - \mu_S^3 - \frac{3\mu_B^2\mu_S}{9} + \frac{6\mu_B\mu_Q\mu_S}{9} - \frac{3\mu_Q^2\mu_S}{9} - \frac{3\mu_B\mu_S^2}{3} + \frac{3\mu_Q\mu_S^2}{3} = 0, \end{aligned} \quad (44)$$

$$\frac{2\mu_B^2\mu_Q}{3} + \frac{2\mu_B\mu_Q^2}{3} + \frac{2\mu_Q^3}{3} - \mu_S^3 - \frac{\mu_B^2\mu_S}{3} + \frac{2\mu_B\mu_Q\mu_S}{3} - \frac{\mu_Q^2\mu_S}{3} - \mu_B\mu_S^2 + \mu_Q\mu_S^2 = 0. \quad (45)$$

In the above expression, we still need to isolate  $\mu_Q$  and replace in Eq. 39.

## References

- Gordon Baym, Tetsuo Hatsuda, Toru Kojo, Philip D. Powell, Yifan Song, and Tatsuyuki Takatsuka. From hadrons to quarks in neutron stars: a review. *Rept. Prog. Phys.*, 81(5):056902, 2018. doi:10.1088/1361-6633/aaae14.
- Mark G. Alford, Andreas Schmitt, Krishna Rajagopal, and Thomas Schäfer. Color superconductivity in dense quark matter. *Rev. Mod. Phys.*, 80:1455–1515, 2008. doi:10.1103/RevModPhys.80.1455.
- Jean Letessier, Ahmed Tounsi, Ulrich W. Heinz, Josef Sollfrank, and Johann Rafelski. Strangeness conservation in hot nuclear fireballs. *Phys. Rev. D*, 51:3408–3435, 1995. doi:10.1103/PhysRevD.51.3408.
- Peng-Cheng Chu and Lie-Wen Chen. Quark matter symmetry energy and quark stars. *Astrophys. J.*, 780:135, 2014. doi:10.1088/0004-637X/780/2/135.
- Lie-Wen Chen. Symmetry Energy in Nucleon and Quark Matter. *Nucl. Phys. Rev.*, 34(1):20–28, 2017. doi:10.11804/NuclPhysRev.34.01.020.
- Xuhao Wu, Akira Ohnishi, and Hong Shen. Effects of quark-matter symmetry energy on hadron-quark coexistence in neutron-star matter. *Phys. Rev. C*, 98(6):065801, 2018. doi:10.1103/PhysRevC.98.065801.
- Suman Thakur and Shashi K. Dhiman. Temperature Effects in Quark Matter Symmetry Free Energy. *DAE Symp. Nucl. Phys.*, 62:696–697, 2017.
- K. Aryal, C. Constantinou, R. L. S. Farias, and V. Dexheimer. High-Energy Phase Diagrams with Charge and Isospin Axes under Heavy-Ion Collision and Stellar Conditions. *Phys. Rev. D*, 102(7):076016, 2020. doi:10.1103/PhysRevD.102.076016.
- Nanxi Yao, Agnieszka Sorensen, Veronica Dexheimer, and Jacquelyn Noronha-Hostler. Structure in the speed of sound: from neutron stars to heavy-ion collisions, 11 2023.
- Adam Burrows and James M. Lattimer. The birth of neutron stars. *Astrophys. J.*, 307:178–196, 1986. doi:10.1086/164405.
- H. David Politzer. Reliable Perturbative Results for Strong Interactions? *Phys. Rev. Lett.*, 30:1346–1349, 1973. doi:10.1103/PhysRevLett.30.1346.
- Tyler Gorda, Alekski Kurkela, Risto Paatelainen, Saga Säppi, and Alekski Vuorinen. Cold quark matter at N3LO: Soft contributions. *Phys. Rev. D*, 104(7):074015, 2021a. doi:10.1103/PhysRevD.104.074015.
- Tyler Gorda, Alekski Kurkela, Risto Paatelainen, Saga Säppi, and Alekski Vuorinen. Soft Interactions in Cold Quark Matter. *Phys. Rev. Lett.*, 127(16):162003, 2021b. doi:10.1103/PhysRevLett.127.162003.
- Alekski Kurkela, Paul Romatschke, and Alekski Vuorinen. Cold Quark Matter. *Phys. Rev. D*, 81:105021, 2010. doi:10.1103/PhysRevD.81.105021.
- Thorben Graf, Juergen Schaffner-Bielich, and Eduardo S. Fraga. The impact of quark masses on pQCD thermodynamics. *Eur. Phys. J. A*, 52(7):208, 2016. doi:10.1140/epja/i2016-16208-9.

Tyler Gorda and Saga Säppi. Cool quark matter with perturbative quark masses. *Phys. Rev. D*, 105(11):114005, 2022. doi:10.1103/PhysRevD.105.114005.

R. L. Workman and Others. Review of Particle Physics. *PTEP*, 2022:083C01, 2022. doi:10.1093/ptep/ptac097.

Bob Holdom, Jing Ren, and Chen Zhang. Quark matter may not be strange. *Phys. Rev. Lett.*, 120(22):222001, 2018. doi:10.1103/PhysRevLett.120.222001.